DEVELOPMENTAL DYNAMICS 242:550–559, 2013

Tbx1 is Required for Second Heart Field Proliferation in Zebrafish

Kathleen Nevis,[1,2] Pablo Obregon,[1,2] Conor Walsh,[1,2] Burcu Guner-Ataman,[1,2] C. Geoffrey Burns,[1,2,3]* and Caroline E. Burns[1,2,3]*

Background: The mammalian outflow tract (OFT) and primitive right ventricle arise by accretion of newly differentiated cells to the arterial pole of the heart tube from multi-potent progenitor cells of the second heart field (SHF). While mounting evidence suggests that the genetic pathways regulating SHF development are highly conserved in zebrafish, this topic remains an active area of investigation. Results: Here, we extend previous observations demonstrating that zebrafish *tbx1* (*van gogh, vgo*) mutants show ventricular and OFT defects consistent with a conserved role in SHF-mediated cardiogenesis. Surprisingly, we reveal through double in situ analyses that *tbx1* transcripts are excluded from cardiac progenitor cells and differentiated cardiomyocytes, suggesting a non-autonomous role in SHF development. Further, we find that the diminutive ventricle in *vgo* animals results from a 25% decrease in cardiomyocyte number that occurs subsequent to heart tube stages. Lastly, we report that although SHF progenitors are specified in the absence of Tbx1, they fail to be maintained due to compromised SHF progenitor cell proliferation. Conclusions: These studies highlight conservation of Tbx1 function in zebrafish SHF biology. *Developmental Dynamics 242:550–559, 2013*. © **2013 Wiley Periodicals, Inc.**

Key words: *tbx1*; zebrafish; heart; second heart field; cardiac

Key Findings:

- Tbx1 is required for second heart field development in zebrafish.
- *Tbx1* transcripts do not overlap with cardiac progenitor cells or differentiated cardiomyocytes during early cardiogenesis in zebrafish.
- First heart field progenitors differentiate normally in *tbx1* mutants.
- Second heart field progenitor specification is largely normal in *tbx1* mutants.
- Second heart field proliferation is severely decreased in *tbx1* mutants.

Accepted 3 January 2013

INTRODUCTION

In higher vertebrates, cardiac crescent cells of the first heart field (FHF) generate the primitive heart tube, which is elongated at both poles by late differentiation of second heart field (SHF) progenitors in pharyngeal mesoderm (Vincent and Buckingham, 2010). At the arterial pole, SHF precursors give rise to new myocardial segments that become the future right ventricle and outflow tract (OFT). Anomolies in OFT development comprise ~30% of congenital heart defects (Srivastava and Olson, 2000) and often result from hemizygous microdeletions in a 3 Mb region on chromosome 22q11.2 (Jerome and Papaioannou, 2001; Lindsay et al., 2001; Merscher et al., 2001). This genomic disruption results in a variable constellation of congenital malformations and cognitive impairments

[1]Cardiovascular Research Center, Massachusetts General Hospital, Harvard Medical School, Charlestown, Massachusetts
[2]Harvard Medical School, Boston, Massachusetts
[3]Harvard Stem Cell Institute, Cambridge, Massachusetts
Grant sponsor: National Institutes of Health; Grant numbers: 5F32HL110627; 5R01HL096816; 5R01HL111179; Grant sponsor: American Heart Association; Grant numbers: 10POST4170037, 10GRNT4270021; Grant sponsor: Harvard Stem Cell Institute; Grant sponsor: March of Dimes Foundation; Grant number: 1-FY12-467.
***Correspondence to: C. Geoffrey Burns/Caroline E. Burns, Cardiovascular Research Center, Massachusetts General Hospital, Harvard Medical School, Charlestown, MA 02129. E-mail: gburns@cvrc.mgh.harvard.edu; cburns6@partners.org**

DOI: 10.1002/dvdy.23928
Published online 17 January 2013 in Wiley Online Library (wileyonlinelibrary.com).

known collectively as DiGeorge Syndrome (DGS). Among the most life-threatening phenotypes are cardiovascular (CV) anomolies, such as Tetralogy of Fallot and Interrupted Aortic Arch, that appear to arise from reduced expression of *TBX1*, a gene in the typically deleted region required for cardiac neural crest and SHF development (Jerome and Papaioannou, 2001; Lindsay et al., 2001; Merscher et al., 2001; Yagi et al., 2003; Xu et al., 2004). Despite the prevalence and severity of CV malformations in the DGS population, ~20% of genetically affected individuals lack any detectable cardiovascular pathology (Ryan et al., 1997). This observation underscores the profound influence of genetic and/or environmental modifiers over the DGS phenotype and reveals the complexity of the requirement for TBX1 in CV development. As such, a more detailed understanding of the molecular mechanisms by which TBX1 influences OFT development are essential.

Much of our understanding of how TBX1 influences CV development comes from gene expression and inactivation studies in the mouse (reviewed in Aggarwal and Morrow, 2008; Parisot et al., 2011; Scambler, 2010). Murine *Tbx1* is expressed in tissues that form the pharyngeal system, including pharyngeal surface ectoderm, pharyngeal endoderm, and pharyngeal mesoderm, which contains SHF progenitors (Chapman et al., 1996; Garg et al., 2001; Jerome and Papaioannou, 2001; Lindsay et al., 2001; Merscher et al., 2001; Vitelli et al., 2002a; Vincent and Buckingham, 2010). In regards to the heart, cre/loxP lineage tracing of *Tbx1*+ cells showed substantial contributions to the inferior myocardial wall and endothelium of the OFT and some contribution to right ventricular myocardium, consistent with *Tbx1* expression in a subset of SHF precursors (Huynh et al., 2007; Xu et al., 2004). Loss-of-function analyses revealed that homozygous *Tbx1* neonates die at birth from severe craniofacial and CV malformations, the latter of which included the loss of the pharyngeal apparatus (pharyngeal arches, pouches, and clefts), OFT hypoplasia, and ventricular septal defects (Jerome and Papaioannou, 2001; Lindsay et al., 2001; Merscher et al., 2001). It has been proposed that TBX1 provides a pro-proliferation signal to SHF progenitors (Chen et al., 2009; Liao et al., 2008; Xu et al., 2004; Zhang et al., 2006b), which is likely mediated, at least in part, by FGF8 (Abu-Issa et al., 2002; Brown et al., 2004; Hu et al., 2004; Park et al., 2006; Vitelli et al., 2010; Vitelli et al., 2002b; Zhang et al., 2006b). This idea is supported by the ability of TBX1 to activate an *Fgf8* enhancer in cell culture (Hu et al., 2004) and by genetic interaction studies between *Tbx1* and *Fgf8* for OFT development in vivo (Brown et al., 2004; Vitelli et al., b,2010; Zhang et al., 2006b).

Why only a fraction of patients hemizygous for a deletion in the *TBX1*-containing region present with DGS while others have no observable abnormalities is not understood. Moreover, the spectrum of defects in affected DGS individuals suggests the existence of genetic or environmental modifiers, most of which are not known. The zebrafish model organism offers distinct strategies for identifying such modifiers, such as forward genetic or small molecule–based screening. Despite being comprised of only two cardiac chambers, the zebrafish heart is partially derived from a SHF population (de Pater et al., 2009; Hami et al., 2011; Lazic and Scott, 2011; Zhou et al., 2011) that expresses *nkx2.5* (Lazic and Scott, 2011; Zhou et al., 2011), *mef2cb* (Hinits et al., 2012; Lazic and Scott, 2011), and *ltbp3* (Zhou et al., 2011). Cre/loxP lineage tracing demonstrated that approximately half of the single ventricular chamber and entire OFT is derived via late differentiation and accretion from SHF progenitors following heart tube formation (Zhou et al., 2011). Impairment of SHF-mediated cardiogenesis results in loss of ventricular cardiomyocytes that normally comprise the distal portion of the chamber and loss or diminution of Elastin2+ (Eln2+) smooth muscle precursor cells of the OFT.

The genetic programs regulating SHF biology in the zebrafish appear largely conserved with that of higher vertebrates. Using small molecule, morpholino, or genetic means of inhibition, FGF (de Pater et al., 2009; Lazic and Scott, 2011; Marques et al., 2008), BMP (Hami et al., 2011), Hedgehog (Hami et al., 2011), and TGFβ (Zhou et al., 2011) signaling have all been implicated as critical SHF pathways in zebrafish. *Islet1* is arguably the best known SHF marker in mice. Despite recent reports suggesting conserved expression of *isl1* in zebrafish SHF progenitors (Hami et al., 2011; Witzel et al., 2012), *isl1*−/− mutants show normal arterial pole development (de Pater et al., 2009). Thus, while evidence of gentic conservation between zebrafish and mammalian SHF-mediated cardiogenesis is mounting, this topic is still an active area of investigation.

In regards to *tbx1*, an initial study in zebrafish showed that *tbx1* null embryos (*van gogh, vgo*) (Piotrowski et al., 2003) have an undersized ventricle, a small Eln2+ smooth muscle component of the outflow tract, and impaired migration of dye-labeled pharyngeal cells into the heart tube (Hami et al., 2011). Taken together, these observations suggest that zebrafish Tbx1 is required for SHF development. However, a more comprehensive characterization of the *vgo* cardiac phenotype is required to determine the degree to which Tbx1 function is conserved. Thus, we sought to confirm and extend initial observations suggesting that Tbx1 function is required for zebrafish SHF development as in mice and presumably humans.

Here, we characterize *tbx1* expression in relation to cardiac progenitors and differentiated cardiomyocytes in zebrafish and analyze *tbx1*/*vgo* null embryos for molecular and morphological evidence of SHF perturbations. Unexpectedly, we found that *tbx1* expression appears non-overlapping with cardiac progenitor cell (CPC) markers of the first and second heart fields or differentiated cardiomyocytes that comprise the early zebrafish heart tube. However, *vgo* mutant ventricles show a clear diminution in size. We discovered that this reduction in ventricular chamber size is due to an approximately 25% decrease in cardiomyocyte number that occurs subsequent to linear heart tube establishment. This finding demonstrates that FHF development proceeds normally in the absence of Tbx1

function, but that SHF development is specifically disrupted. Further, we discovered that the SHF defect in *vgo* mutants is caused by compromised SHF progenitor cell proliferation. Overall, our data suggest that *Tbx1* function during SHF development is conserved in zebrafish.

RESULTS

Although the developmental expression pattern of zebrafish *tbx1* has been reported previously (Kochilas et al., 2003; Piotrowski et al., 2003; Zhang et al., 2006a), we sought to characterize the location of *tbx1* transcripts relative to cardiac markers during zebrafish cardiogenesis. First, we performed double in situ hybridization prior to early myocardial differentiation with *tbx1* and the conserved cardiac progenitor marker *nkx2.5*. At the 8 somites-stage [8ss; 13 hours post-fertilization (hpf)], *tbx1* transcripts are located in regions both medial (Fig. 1A–C) and dorsal (Fig. 1C,D) to *nkx2.5*+ CPCs. Interestingly, *fgf8a* transcripts were reported to have a similar dorsomedial relationship with *nkx2.5* at similar developmental stages (Reifers et al., 2000). Cross-section analysis provided further evidence that *tbx1* expression is non-overlapping with *nkx2.5* (Fig. 1C). Next, we examined the localization of *tbx1* transcripts relative to a cardiomyocyte marker, *cardiac myosin light chain 2* (*cmlc2*; also called *myl7*) (Yelon et al., 1999) and the SHF marker *latent TGF-β binding protein 3* (*ltbp3*) (Zhou et al., 2011). At 16ss (17hpf), *cmlc2* transcripts mark FHF-derived myocardial cells in the anterior lateral plate mesoderm (ALPM) (de Pater et al., 2009; Lazic and Scott, 2011). At this stage, *tbx1* transcripts were observed lateral to the medially migrating *cmlc2*+ cardiomyocytes of the heart-forming region (Fig. 1E). Similarly at 23ss (20.5hpf), *tbx1* transcripts were readily visible in the developing pharyngeal arches (Piotrowski et al., 2003), but absent from *cmlc2*+ cells that comprise the cardiac cone (Fig. 1F), a precursor to the linear heart tube in zebrafish. At the same developmental stage, *ltbp3* expression commenced in SHF progenitors but failed to overlap spatially with *tbx1* (Fig. 1G). Finally, after establishment of the linear heart tube (24hpf), *tbx1* transcripts were absent from the heart tube proper (Fig. 1H) and its arterial pole inhabited by SHF progenitor cells (Fig. 1H, inset) (Hami

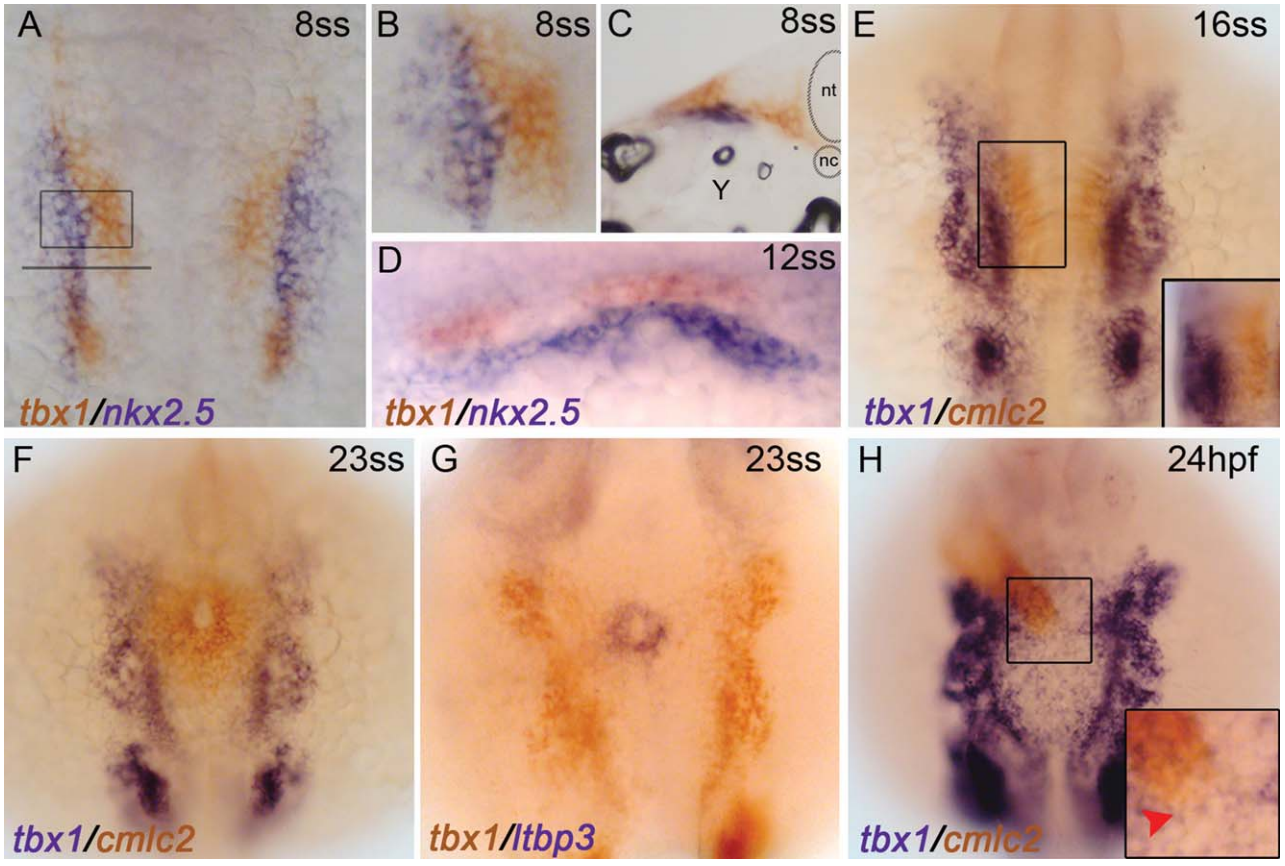

Fig. 1. *tbx1* transcripts do not co-localize with CPCs or cardiomyocytes during early cardiogenesis in zebrafish. Whole-mount double in situ hybridizations are shown. A–D: *tbx1* (red) and *nkx2.5 (*blue) transcripts are non-overlapping at 8ss and 12ss. **A:** Flat mount, dorsal view, anterior up, 10× maginification. **B:** 20× magnification of the ALPM (boxed region in A). **C:** Transverse cryo-section, through the left ALPM (location of section shown by the solid line in A), 20× magnification, nt = neural tube, nc = notochord, Y = yolk. **D:** Dorso-lateral view showing that *tbx1*-expressing cells reside dorsal to *nkx2.5*-expressing CPCs at 12ss. **E,F:** *tbx1*$^{+}$ cells are lateral to *cmlc2*+ cardiomyocytes at 16ss and 23ss. Dorsal view, anterior up, 10× magnification. Inset is 20× magnification of the boxed region photographed from a more dorsolateral view. **G:** *tbx1*$^{+}$ cells are lateral to *ltbp3*+ SHF progenitors at 20.5hpf/23ss. Dorsal view, anterior up, 10× magnification. **H:** At 24hpf, the linear heart tube resides dorsal to the *tbx1* expression domain in different planes of focus. Dorsal view, anterior up, 10× magnification. *tbx1* is not expressed at the arterial pole of the linear heart tube where SHF progenitors reside (red arrowhead). Inset is 20× magnification of boxed region.

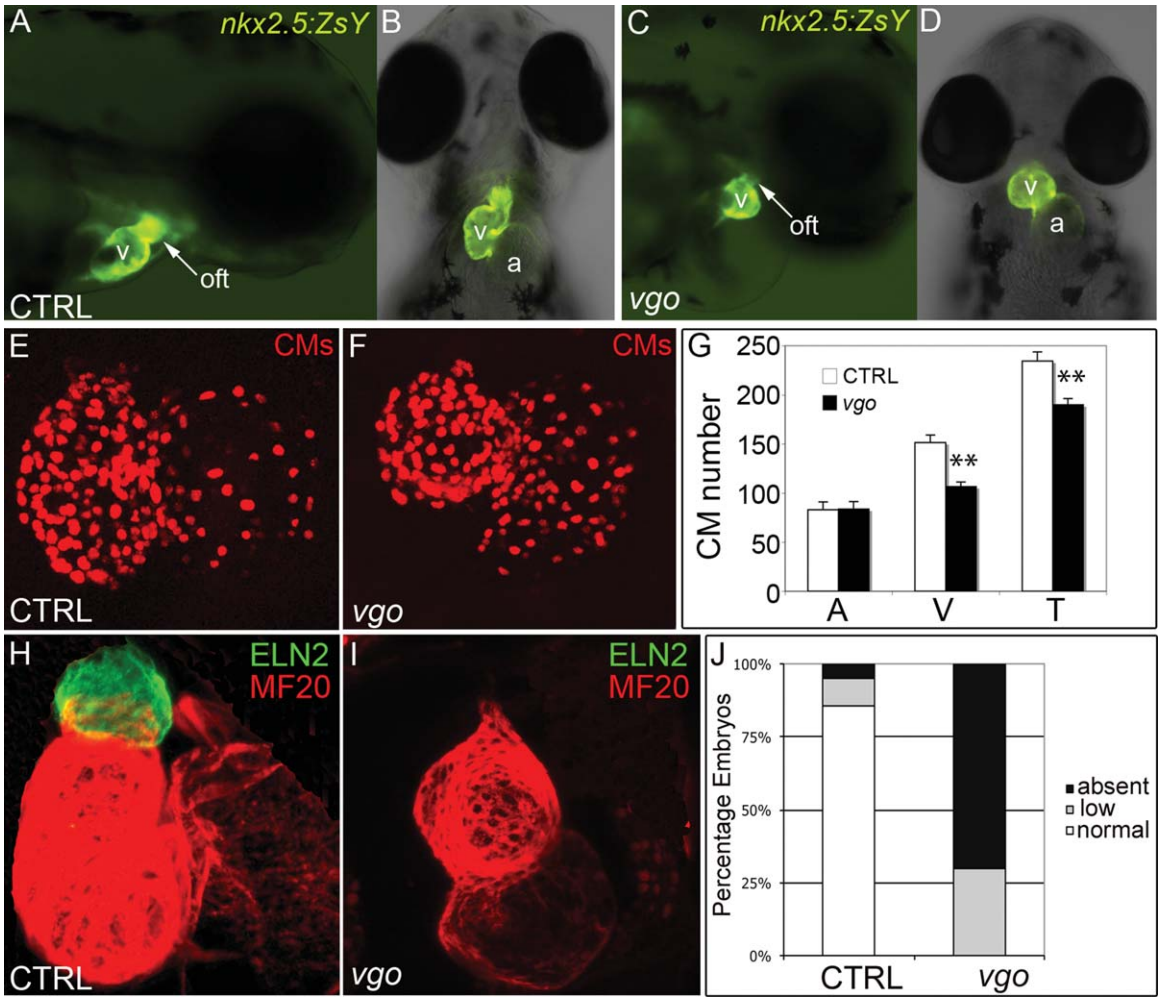

Fig. 2. *tbx1* mutants display diminutive ventricles caused by decreased cardiomyocyte numbers and diminished OFT smooth muscle. **A–D:** Fluorescence microscopy images of *Tg(nkx2.5:ZsYellow)* control (CTRL) and *vgo* embryos; 10× magnification. At 72 hpf, the ventricular chamber and OFT appears small in *vgo* (C,D) compared to control (A,B). A,C: Lateral view, anterior right. B,D: Ventral view, anterior up. v = ventricle, a = atrium, oft = outflow tract. **E,F:** Flattened confocal images of cardiomyocyte (CM) nuclei in 72hpf *Tg(cmlc2::DsRed^{nuc})* control (E) and *vgo* (F) hearts. **G:** Graph depicting the average number of CMs at 72hpf in control (n=4) and *vgo* (n=4) embryos. Asterisks indicate statistical significance as determined using unpaired Student's *t*-test. Error bars represent +/− 1s.e.m. Atrial (A) CM numbers remain unchanged (P=0.47), while ventricular (V) and total (T) CM numbers are significantly lower in *vgo* mutants (P=0.00008 and 0.0002, respectively). **H,I:** Flattened confocal images following double immunofluorescence to visualize OFT smooth muscle precursors (Eln2; green) and chamber cardiomyocytes (MF20; red) in 72 hpf control (n=21; H) and *vgo* (n=20; I) embryos. **J:** Graph depicting the percentages of control or *vgo* embryos with normal low, or absent Eln2 staining.

et al., 2011; Lazic and Scott, 2011; Zhou et al., 2011). Taken together, these data suggest that zebrafish *tbx1* transcripts are non-overlapping with CPC markers and differentiated cardiomyocytes that comprise the early zebrafish heart tube.

To determine if zebrafish embryos devoid of *tbx1* display evidence of defective cardiogenesis, we analyzed embryos homozygous for the *tbx1* null alleles, *van gogh^{tu285}* (*vgo^{tu285}*) and *van gogh^{tu208}* (*vgo^{tu208}*), which produce indistinguishable embryonic phenotypes (Piotrowski et al., 2003; Piotrowski and Nusslein-Volhard, 2000). To visualize cardiogenesis in the absence of *tbx1*, we crossed the *vgo^{tu285}* allele with a previously described *Tg(nkx2.5:ZsYellow)^{fb7}* transgenic line that reports yellow fluorescence in *nkx2.5+* cells (henceforth called *nkx2.5:ZsY*) (Zhou et al., 2011). Consistent with a previous report (Hami et al., 2011), we observed a diminuitive ventricle in *vgo* mutants compared to controls at 72hpf (Fig. 2A–D), a timepoint following SHF-mediated myocardial accretion (de Pater et al., 2009; Hami et al., 2011; Lazic and Scott, 2011; Zhou et al., 2011). This size difference could be due to a decrease in the number of ventricular cardiomyocytes or equivalent numbers of ventricular cells that are smaller and more densely organized. To distinguish between these alternatives, we quantified the number of cardiomyocytes in each chamber of control and *vgo^{tu285}* mutant embryos at 72hpf using a transgenic strain in which cardiomyocyte nuclei express DsRed2 fluorescent protein (Mably et al., 2003). From this analysis, we learned that *vgo* embryos display no alterations in the number of atrial cells but exhibit an approximately 25% decrease in the number of ventricular cardiomyocytes compared to controls (Fig. 2E–G). Moreover, OFT smooth muscle precursors marked by Elastin2 (Eln2) (Miao et al., 2007; Grimes et al., 2006) were severely diminished or absent in *vgo*

embryos compared to control siblings (Fig. 2H–J). Together, these data demonstrate that the small ventricle phenotype observed in *vgo* mutants results from a ventricular cardiomyocyte deficit and suggests that *tbx1* function is essential for zebrafish SHF development.

A decrease in the number of ventricular cardiomyocytes could arise from a defect in FHF-mediated cardiogenesis. Therefore, we compared the spatial and temporal expression of cardiac markers at the cone stage (23ss/20.5hpf), a timepoint prior to SHF-mediated myocardial accretion, between vgo^{tu285} and sibling embryos. At 23ss, *nkx2.5:ZsY* reporter fluorescence (Fig. 3A,B) and *ventricular myosin heavy chain* (*vmhc*) transcripts (Fig. 3C,D), which together highlight differentiated FHF-derived ventricular cardiomyocytes and undifferentiated SHF progenitors (Yelon at al., 1999; Schoenbeck et al., 2007; Lazic and Scott, 2011; Zhou et al., 2011), appeared grossly normal in *vgo* animals. Next, we quantified the numbers of cardiomyocytes in the FHF-derived linear heart tubes of control and *vgo* embryos. We found that although the heart tube of *vgo* animals appeared somewhat misshapen compared to their sibling controls, the total number of cardiomyocytes was similar (Fig. 3E–G). These data provide conclusive evidence that FHF-derived cardiogenesis is unaffected in *vgo* mutants, formally demonstrating that the ventricular phenotype observed is not due to compromised FHF development.

Recently, we and others have demonstrated that zebrafish cardiogenesis relies on a second heart field (SHF) that resides in pharyngeal mesoderm and accretes myocardium to the arterial pole of the linear heart tube (de Pater et al., 2009; Hami et al., 2011; Lazic and Scott, 2011; Zhou et al., 2011). The molecular signature of the zebrafish SHF to date is *nkx2.5, mef2cb,* and *ltbp3*. *ltbp3* is the most specific marker spatiotemporally of the SHF in zebrafish (Zhou et al., 2011; Lazic and Scott, 2011). To determine if the ventricular deficit in vgo^{tu285} mutants is a result of perturbations in *ltbp3* expression, we performed in situ hybridization using an *ltbp3* riboprobe at progressive developmental stages. At 23ss (20.5hpf), when *ltbp3* transcripts are first visualized by in situ analyses, we learned that *ltbp3* expression was properly initiated in *vgo* embryos (Fig. 4A,B). However, at the linear heart tube stage (24hpf), *ltbp3* transcripts were no longer detected in SHF progenitors in *vgo* mutants (Fig. 4C,D). We confirmed the absence of SHF precursors at heart tube stages in vgo^{tu208} embryos using a complementary approach that relies on the fluorescent reporter transgenic strains *Tg(nkx2.5:ZsY)* and *Tg(cmlc2:GFP)*. To distinguish the two fluorophores by confocal microscopy, double fluorescent immunohistochemistry was performed to highlight

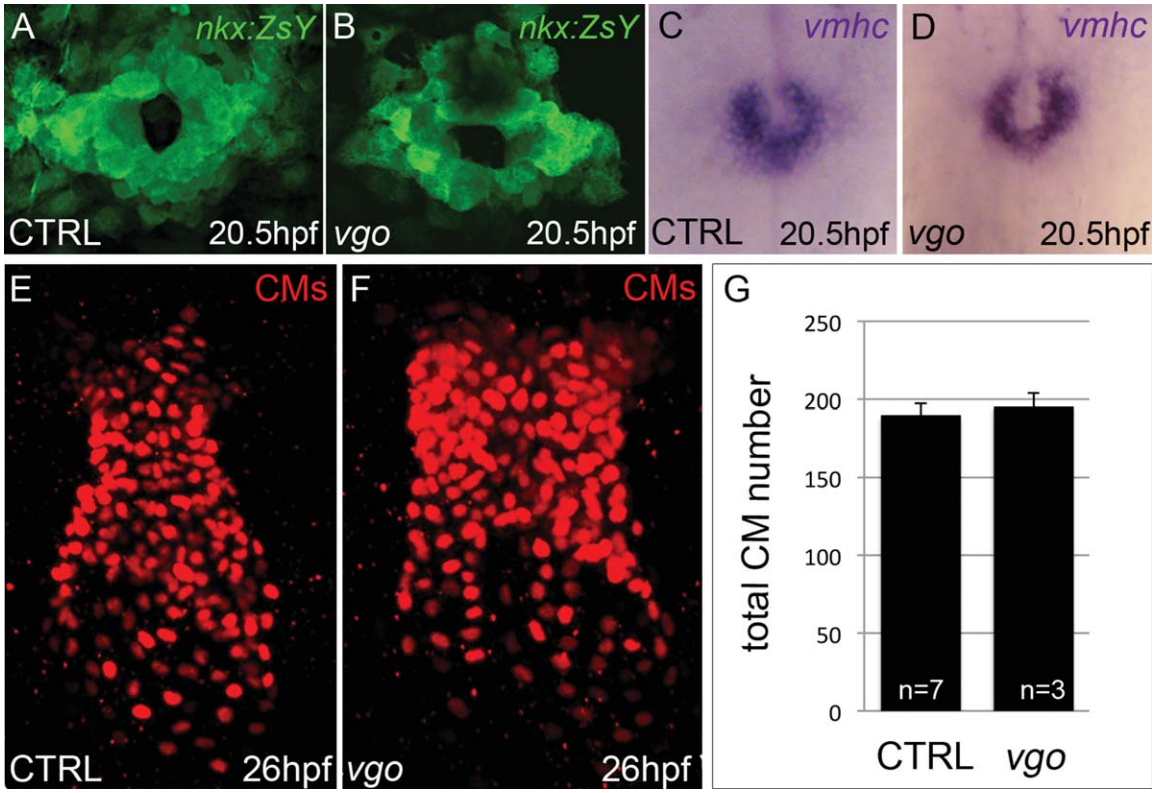

Fig. 3. FIrst heart field development is unaffected in *tbx1* mutants. **A,B:** Flattened confocal images of *Tg(nkx2.5::ZsYellow)* control (n=37; A) and *vgo* (n=14; B) embryos at 20.5hpf/23ss. **C,D:** Whole-mount in situ hybridization of *vmhc* at 20.5hpf/23ss in both control (n=16; C) and *vgo* (n=16; D) embryos. **E,F:** Flattened confocal images following immunofluorescence of cardiomyocyte nuclei comprising the linear heart tubes of 26 hpf control (E) and *vgo* (F) *Tg*(*cmlc2:dsRed2-nuc*) embryos. Dorsal view, anterior up in all images. **G:** Graph depicting the average number of CMs at 26 hpf in control and *vgo* embryos.

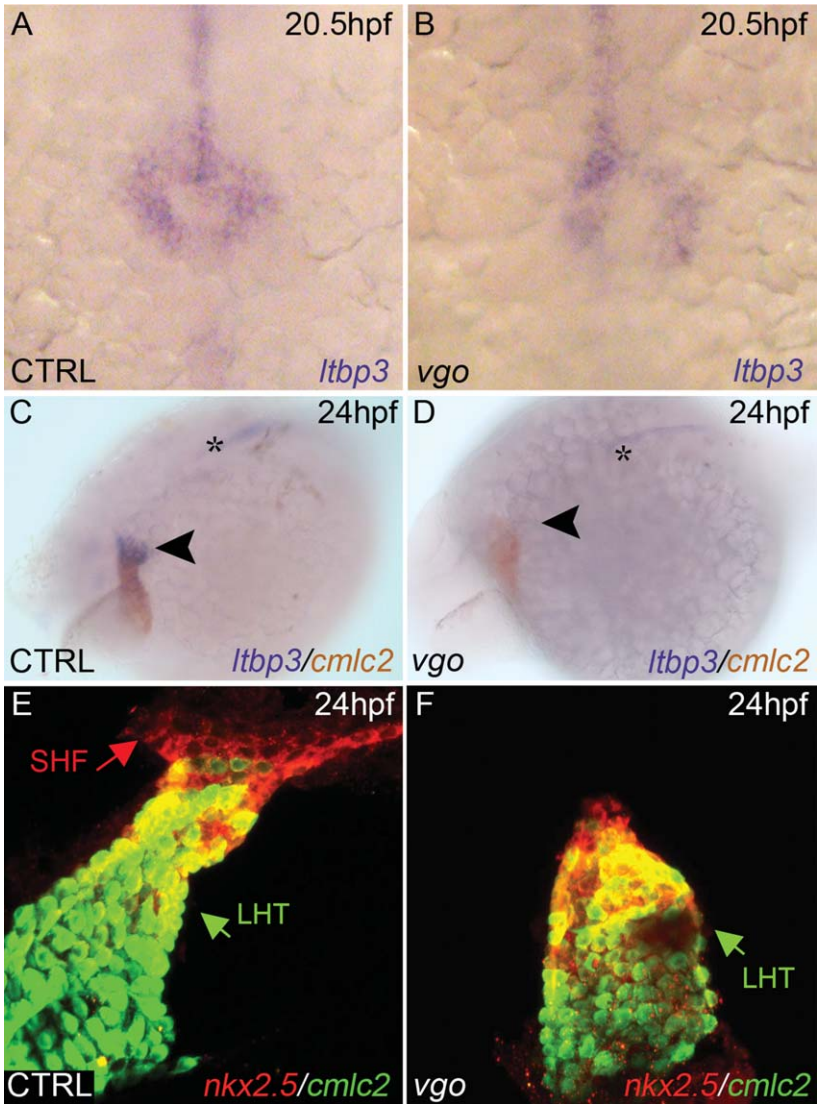

Fig. 4. Initial specification of SHF progenitors is not perturbed in vgo embryos. **A,B:** *ltbp3* was observed via whole-mount in situ hybridization at 20.5hpf/23ss in control (A) and *vgo* (B) embryos (n>12). Dorsal view, anterior down. 20× magnification. **C,D:** Whole-mount double in situ hybridization at 26 hpf shows *ltbp3*$^{+}$ (blue) cells at the arterial pole (arrowhead) of the *cmlc2*$^{+}$ (red) heart tube in control embryos. *ltbp3* expression is drastically reduced (21%) or absent (79%) at the arterial pole of *vgo* hearts (n=14). Asterisk indicates *ltbp3* expression within the notochord. **E,F:** At 26hpf, double transgenic *Tg(nkx2.5::ZsYellow); Tg(cmlc2::GFP)* control (E) and *vgo* (F) embryos were co-immunostained with GFP antibody (anti-GFP, green) and ZsYellow antibody (anti-RCFP, red). The future atrial segment of the linear heart tube (LHT, green arrow) expresses *cmlc2* alone (green), while the future proximal ventricular myocardium co-expresses *cmlc2* and *nkx2.5* (yellow). Non-myocardial *nkx2.5*+ second heart field (SHF) progenitors (red arrow) can be visualized in control animals (n=8), but are lacking in *vgo* mutants (n=7).

cmlc2+ differentiated cardiomyocytes in green and *nkx2.5*+ SHF progenitors and differentiated ventricular cardiomyocytes in red. Although a distinct *nkx2.5*+ population of SHF progenitors could be easily visualized at the arterial pole of the heart tube at 24–26 hpf in control embryos, this population was absent in *vgo* mutants (Fig. 4E,F). Together, these data suggest that SHF specification is largely unperturbed in vgo embryos.

To elucidate the cellular mechanisms underlying the *vgo* SHF phenotype, we evaluated mutants soon after cardiac cone stages for cellular defects in the extra-cardiac population of *nkx2.5*+ SHF cells at the arterial pole. First, we used TUNEL (terminal deoxynucleotidyl transferase biotin-dUTP nick end-labeling) labelling to highlight apoptotic cells in control and *vgo*^{tu285} mutants carrying the *nkx2.5:ZsY* transgene. Although TUNEL+ apoptotic cells were observed throughout the bodies of both control and *vgo* embryos, no TUNEL+ cells were detected in the *ZsY*+ SHF domain (data not shown). Next, we used the thymidine analog EdU to examine proliferation of *nkx2.5:ZsY*+ SHF cells at the arterial pole. Specifically, embryos were pulsed with 5-ethynyl-2′deoxyuriding (EdU) at 20ss (19 hpf) and collected at 26ss (22hpf) for double staining with antibodies to detect EdU incorporation and ZsYellow. We detected extensive proliferation throughout the bodies of both *vgo*^{tu285} and sibling controls (Fig. 5A,B). Interestingly, we observed abundant proliferative ZsY+ cells that predominantly localized to the arterial pole/SHF region of the cardiac cone (Fig. 5C,E). However, while the cardiac cone appeared similar between *vgo* and sibling controls (Fig. 5A,B, insets), a significant decrease in the number of proliferative EdU+ SHF progenitors was observed in *vgo* mutants (Fig. 5C–E). These findings support a model in which Tbx1 stimulates proliferation or self-renewal of *ltpb3+; nkx2.5*+ SHF progenitors to maintain the CPC pool as new myocardium is accreted to the linear heart tube. Based on this model, we speculate that loss of Tbx1 results in a premature depletion of undifferentiated CPCs from the SHF.

DISCUSSION

Because SHF perturbations are predicted to be common causes of conotruncal malformations in patients, studies designed to decipher the molecular regulation of SHF biology are significant. Specifically, any gene implicated in SHF development becomes a candidate that, when mutated, may cause OFT-related congenital heart defects. Mounting evidence suggests that the genetic pathways regulating SHF development are highly conserved in zebrafish. Here, we confirm and extend previous findings (Hami et al., 2011) that *tbx1* is required for SHF development in zebrafish. These studies serve to further solidify the use of the zebrafish

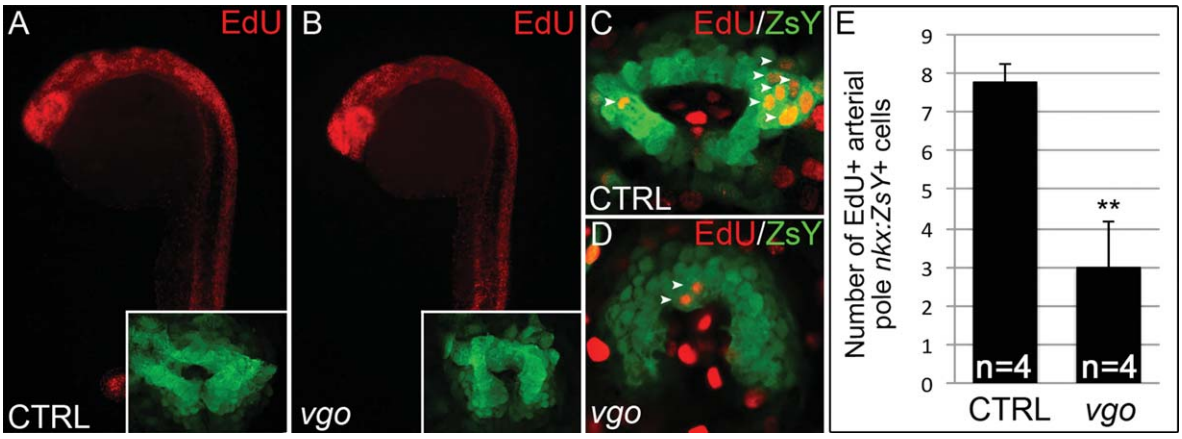

Fig. 5. SHF progenitor cells fail to proliferate in the absence of Tbx1. A–D: Click-iT EdU labeling in 23ss *Tg(nkx2.5:ZsYellow) vgo* and control siblings. **A,B:** Flourescence microscopy images of EdU+ cells (red) in control (A) and *vgo* (B) embryos. 10× magnification, anterior up, dorsal right. Insets show flattened confocal images of *ZsY*+ cells comprising the cardiac cone. **C,D:** Composites of two confocal sections showing EdU+ cells (red) within the ZsYellow+ (green) SHF (white arrowheads). **E:** Graph depicting the average total numbers of EdU+, ZsYellow+ cells in confocal stacks of control (n=4) and *vgo* (n=4) embryos.

model organism for discovery-based approaches that may uncover new and potentially clinically relevant genes controlling arterial pole development.

Deciphering the tissue-specific roles of TBX1 in mammalian OFT morphogenesis has been extremely complex due in part to the high degree of interaction between the *Tbx1*-expressing pharyngeal endoderm and pharyngeal mesoderm, the latter of which contains SHF progenitors. While conditional loss-of-function studies have yielded valuable information, the interpretations have been clouded by cre-mediated recombination in both tissue compartments. For example, although deletion of *Tbx1* in the *Nkx2.5* expression domain results in OFT hypoplasia, recombination occurs in the pharyngeal endoderm, pharyneal mesoderm, and SHF (Xu et al., 2004, 2005). In another study, Arnold et al. showed that deletion of *Tbx1* in the *Foxg1*+ pharyngeal endoderm results in severe OFT defects that resemble those occurring in *Tbx1*−/− nulls (Arnold et al., 2006). Although *Foxg1*-mediated recombination was reported to be limited to pharyngeal endoderm in this study (Arnold et al., 2006), Zhang et al. observed additional *Foxg1*-induced cre activity in pharyngeal mesoderm when examining recombination on a different genetic background (Zhang et al., 2005). Thus, the specific interplay between the pharyngeal endoderm and mesoderm in regards to mouse TBX1 function remains unclear.

The most compelling argument that TBX1 functions cell non-autonomously for SHF development in the mouse comes from mosaic analyses (Xu et al., 2004). Specifically, *Tbx1*−/− cells were mixed with wild-type cells to generate embryos of mixed genetic origin. In these mice, *Tbx1*−/− cells contributed to the SHF, showed no proliferative disadvantage, and were accreted at the same frequency as wild-type cells to the developing OFT. Interestingly, inactivation of *Tbx1* in *Mesp1*+ mesoderm results in severe OFT defects that can be rescued by mesodermal restoration of *Tbx1* (Zhang et al., 2006b). Although these data show a strict requirement for *Tbx1* in the mesoderm, *Mesp1* is expressed rather broadly leaving open the possibility that *Tbx1* is required in a mesodermal population distinct from the SHF. Thus, the outcome of these lineage-specific inactivation/reactivation experiments remains consistent with those from the chimera analyses that demonstrated a non-autonomous role for TBX1 in SHF-mediated OFT formation.

Our studies in zebrafish show that Tbx1 is required for SHF proliferation and, based on its expression pattern, most likely acts cell non-autonomously. Although our in situ analyses are unable to definitively exclude *tbx1* expression in medial *nkx2.5*+ cells in the heart-forming region, which may represent SHF progenitors, the domains appear separate. Moreover, we failed to observe transcripts in the region occupied by SHF progenitors at cardiac cone or heart tube stages. Our observations coupled with previous reports showing *tbx1* transcripts in the pharynx (Piotrowski et al., 2003) makes it tempting to speculate that perhaps the role of Tbx1 in pharyngeal tissues has been conserved in zebrafish for OFT development. However, chimera analyses to determine autonomy in OFT development and cre/loxP-mediated genetic lineage tracing of *tbx1*-expressing cells in zebrafish will be required to appreciate the complete *tbx1* expression profile and tissue derivatives during cardiac development.

Although *tbx1* does not appear to be expressed in SHF progenitors in zebrafish, our data and that of Hami et al. (2011) show that Tbx1 is required for SHF development. Experimental evidence garnered from *ltbp3* cre/loxP lineage tracing (Zhou et al., 2011) and a photoconversion assay that measures the timing of cardiomyocyte differentiation (Lazic and Scott, 2011) suggests that approximately 40–50% of the ventricular chamber is derived from SHF progenitors following heart tube formation. However, our ventricular cardiomyocyte counts in *tbx1* mutants revealed only a 25% reduction. This outcome could be explained several ways. It is possible

that only 25% of the ventricle is derived from SHF cells and that our previous cre/loxP lineage tracing overestimated the contribution made by the SHF as *ltbp3* expression partially overlaps with differentiated cardiomyocytes at the end of the heart tube. Alternatively, because *ltbp3* expression is initiated in *tbx1* null animals, it is possible that there is only a partial myocardial deficit in *vgo* animals. Another explanation, which is consistent with its role in the mouse (Parisot et al., 2011), is that Tbx1 is required for proper development of a sub-domain within a larger SHF. As new SHF markers and lineage traces emerge in zebrafish, a better understanding of the full complement of cardiovascular derivatives of the SHF will be revealed, ultimately aiding our understanding of mutant phenotypes and gene function.

EXPERIMENTAL PROCEDURES

Zebrafish Lines and Maintenance

Zebrafish embryos, larvae, and adults were produced, grown, and maintained according to standard protocols approved by the Institutional Animal Care and Use Committees of Massachusetts General Hospital. Ethical approval was obtained from the Institutional Animal Care and Use Committees of Massachusetts General Hospital. The previously published vgo^{tu285} and vgo^{tu208} mutant *tbx1* alleles were used in this study (Piotrowski et al., 1996, 2003; Schilling et al., 1996). The vgo^{285} and vgo^{208} alleles of *tbx1* contain a C → T and an A → T transition at nucleotide positions 364 and 879, respectively, each creating premature stop codons. Transgenic strains *Tg(cmlc2::DsRed-nuc)* (Mably et al., 2003), *Tg(nkx2.5::ZsYellow)* (Zhou et al., 2011), and *Tg(cmlc2::GFP)* (Burns et al., 2005) were described previously.

Double In Situ Hybridization, Immunohistochemistry, and Cryosectioning

Single and double in situ hybridizations were performed as described (Thisse et al., 1993), with digoxygenin-labeled antisense RNA probes to *ltbp3* (EcoRI/Sp6), *nkx2.5*(EcoRI/T7), *tbx1* (EcoRI/T7), *vmhc* (EcoRI/T3), and fluorescein-labeled antisense RNA probes to *cmlc2* (NotI/T7) and *tbx1*. For cryo-sections, stained embryos were washed in PBS and embedded in 1.2% agarose in a 5% sucrose solution. Embedded embryos were placed in 30% sucrose solution overnight at 4°C. Agarose blocks were covered with Optimal Cutting Temperature compound (OCT) (Tissue-Tek, Torrance, CA) and 50-μm sections were taken using Leica CM 3050 S cryostat. Immunohistochemistry was performed as described (Zhou et al., 2011), using primary antibodies anti-GFP mouse mono-clonal (1:50; Santa Cruz Biotechnology, Santa Cruz, CA), anti-RCFP rabbit polyclonal pan (1:50; Clontech, Mountain View, CA), anti-dsRed rabbit polyclonal (1:50; Clontech), muscle-specific MF20 (1:50; University of Iowa, Iowa City, IA), Elastin-2 (1:1,000; Fred Keeley) and secondary antibodies Alexa Fluor 555 goat anti-rabbit IgG_{2b}, Alexa Fluor 488 goat anti-mouse IgG_{2b}, and Alexa Fluor 546 goat anti-mouse IgG_{2b} (all 1:200; Invitrogen, Carlsbad, CA).

Bright Field, Fluorescence, and Confocal Microscopy

Confocal imaging was performed as described previously (Zhou et al., 2011) on a LS5 confocal microscope (Zeiss, Thornwood, NY) using a 40× water immersion objective. ImageJ (v1.43U; National Institute of Health, Bethesda, MD) software was used to count cardiomyocyte (CM) nuclei in Z-stack confocal images. Statistical significance for CM counts was determined using unpaired Student's t-test. Bright field and fluorescent microscopy was performed with a 10× objective on an Eclipse 80i microscope (Nikon, Melville, NY) using a Retiga 2000R camera (Q-imaging, Surrey, BC Canada) and NIS-Elements AR 3.00 imaging software (Nikon).

TUNEL and Click-iT EdU Staining

TUNEL (terminal deoxynucleotidyl transferase biotin-dUTP nick end-labeling) was performed as described previously (Zhou et al., *2011*). Briefly, *Tg*(*nkx2.5:ZsYellow*) vgo^{285} mutant and control embryos were collected at 23ss and fixed overnight at 4°C in 4% paraformaldehyde before being transferred to 100% methanol and stored at −20°. Embryos were rehydrated in methonol/PBST series, permeabilized with proteinase K, and subjected to a TUNEL assay via the In Situ Cell Death Detection Kit, TMR red (Roche Applied Science, Indianapolis, IN) according to the manufacturer's instructions. Proliferation experiments were performed as previously described (Mahler et al., 2010) using the Click-iT EdU imaging kit (Invitrogen, Carlsbad, CA). Briefly, embryos were incubated on ice for 30 min in 10 mM 5-ethynyl-2′deoxyuriding (EdU), rinsed 3 times in embryo medium, and chased for 3 hr at 28°C. Immunofluorescent staining with anti-rCFP (Alexa-488) and Click-iT-Alexa-555 was performed and embryos were analyzed using confocal microscopy.

ACKNOWLEDGMENTS

We thank L. Zon and I. Scott for providing zebrafish strains; J Holzschuh for providing a detailed Click-iT EdU labeling protocol; Fred Keeley for providing Elastin2 anti-serum; and the Developmental Studies Hybridoma Bank under the auspices of the NICHD and maintained by the University of Iowa, Department of Biological Sciences, Iowa City, IA 52242, for providing the MF20 antibody. This work was supported by awards from the National Institutes of Health to K.N. (5F32HL110627); the American Heart Association to B.G-A. (10POST-4170037); the American Heart Association (Grant in Aid no. 10GRNT-4270021); the Harvard Stem Cell Institute (Seed Grant), and the National Heart Lung and Blood Institute (5R01HL-096816) to C.G.B; and the Harvard Stem Cell Institute (Young Investigator Award and Cardiovascular Program Award), National Heart Lung and Blood Institute (5R01HL111179), and the March of Dimes Foundation (1-FY12-467) to C.E.B.

REFERENCES

Abu-Issa R, Smyth G, Smoak I, Yamamura K, Meyers EN. 2002. Fgf8 is

required for pharyngeal arch and cardiovascular development in the mouse. Development 129:4613–4625.

Aggarwal VS, Morrow BE. 2008. Genetic modifiers of the physical malformations in velo-cardio-facial syndrome/DiGeorge syndrome. Dev Disabil Res Rev 14:19–25.

Arnold JS, Werling U, Braunstein EM, Liao J, Nowotschin S, Edelmann W, Hebert JM, Morrow BE. 2006. Inactivation of Tbx1 in the pharyngeal endoderm results in 22q11DS malformations. Development 133:977–987.

Brown CB, Wenning JM, Lu MM, Epstein DJ, Meyers EN, Epstein JA. 2004. Cre-mediated excision of Fgf8 in the Tbx1 expression domain reveals a critical role for Fgf8 in cardiovascular development in the mouse. Dev Biol 267:190–202.

Burns CG, Milan DJ, Grande EJ, Rottbauer W, MacRae CA, Fishman MC. 2005. High-throughput assay for small molecules that modulate zebrafish embryonic heart rate. Nat Chem Biol 1:263–264.

Chapman DL, Garvey N, Hancock S, Alexiou M, Agulnik SI, Gibson-Brown JJ, Cebra-Thomas J, Bollag RJ, Silver LM, Papaioannou VE. 1996. Expression of the T-box family genes, Tbx1-Tbx5, during early mouse development. Dev Dyn 206:379–390.

Chen L, Fulcoli FG, Tang S, Baldini A. 2009. Tbx1 regulates proliferation and differentiation of multipotent heart progenitors. Circ Res 105:842–851.

de Pater E, Clijsters L, Marques SR, Lin YF, Garavito-Aguilar ZV, Yelon D, Bakkers J. 2009. Distinct phases of cardiomyocyte differentiation regulate growth of the zebrafish heart. Development 136:1633–1641.

Garg V, Yamagishi C, Hu T, Kathiriya IS, Yamagishi H, Srivastava D. 2001. Tbx1, a DiGeorge syndrome candidate gene, is regulated by sonic hedgehog during pharyngeal arch development. Dev Biol 235:62–73.

Grimes AC, Stadt HA, Shepherd IT, Kirby ML. 2006. Solving an enigma: arterial pole development in the zebrafish heart. Dev Biol 290:265–276.

Hami D, Grimes AC, Tsai HJ, Kirby ML. 2011. Zebrafish cardiac development requires a conserved secondary heart field. Development 138:2389–2398.

Hinits Y, Pan L, Walker C, Dowd J, Moens CB, Hughes SM. 2012. Zebrafish Mef2ca and Mef2cb are essential for both first and second heart field cardiomyocyte differentiation. Dev Biol 369:199–210.

Hu T, Yamagishi H, Maeda J, McAnally J, Yamagishi C, Srivastava D. 2004. Tbx1 regulates fibroblast growth factors in the anterior heart field through a reinforcing autoregulatory loop involving forkhead transcription factors. Development 131:5491–5502.

Huynh T, Chen L, Terrell P, Baldini A. 2007. A fate map of Tbx1 expressing cells reveals heterogeneity in the second cardiac field. Genesis 45:470–475.

Jerome LA, Papaioannou VE. 2001. DiGeorge syndrome phenotype in mice mutant for the T-box gene, Tbx1. Nat Genet 27:286–291.

Kochilas LK, Potluri V, Gitler A, Balasubramanian K, Chin AJ. 2003. Cloning and characterization of zebrafish tbx1. Gene Expr Patterns 3:645–651.

Lazic S, Scott IC. 2011. Mef2cb regulates late myocardial cell addition from a second heart field-like population of progenitors in zebrafish. Dev Biol 354:123–133.

Liao J, Aggarwal VS, Nowotschin S, Bondarev A, Lipner S, Morrow BE. 2008. Identification of downstream genetic pathways of Tbx1 in the second heart field. Dev Biol 316:524–537.

Lindsay EA, Vitelli F, Su H, Morishima M, Huynh T, Pramparo T, Jurecic V, Ogunrinu G, Sutherland HF, Scambler PJ, Bradley A, Baldini A. 2001. Tbx1 haploinsufficieny in the DiGeorge syndrome region causes aortic arch defects in mice. Nature 410:97–101.

Mably JD, Mohideen MA, Burns CG, Chen JN, Fishman MC. 2003. heart of glass regulates the concentric growth of the heart in zebrafish. Curr Biol 13:2138–2147.

Mahler J, Filippi A, Driever W. 2010. DeltaA/DeltaD regulate multiple and temporally distinct phases of notch signaling during dopaminergic neurogenesis in zebrafish. J Neurosci 30:16621–16635.

Marques SR, Lee Y, Poss KD, Yelon D. 2008. Reiterative roles for FGF signaling in the establishment of size and proportion of the zebrafish heart. Dev Biol 321:397–406.

Merscher S, Funke B, Epstein JA, Heyer J, Puech A, Lu MM, Xavier RJ, Demay MB, Russell RG, Factor S, Tokooya K, Jore BS, Lopez M, Pandita RK, Lia M, Carrion D, Xu H, Schorle H, Kobler JB, Scambler P, Wynshaw-Boris A, Skoultchi AI, Morrow BE, Kucherlapati R. 2001. TBX1 is responsible for cardiovascular defects in velo-cardio-facial/DiGeorge syndrome. Cell 104:619–629.

Miao M, Bruce AE, Bhanji T, Davis EC, Keeley FW. 2007. Differential expression of two tropoelastin genes in zebrafish. Matrix Biol 26:115–124.

Parisot P, Mesbah K, Theveniau-Ruissy M, Kelly RG. 2011. Tbx1, subpulmonary myocardium and conotruncal congenital heart defects. Birth Defects Res A Clin Mol Teratol 91:477–484.

Park EJ, Ogden LA, Talbot A, Evans S, Cai CL, Black BL, Frank DU, Moon AM. 2006. Required, tissue-specific roles for Fgf8 in outflow tract formation and remodeling. Development 133:2419–2433.

Piotrowski T, Nusslein-Volhard C. 2000. The endoderm plays an important role in patterning the segmented pharyngeal region in zebrafish (*Danio rerio*). Dev Biol 225:339–356.

Piotrowski T, Schilling TF, Brand M, Jiang YJ, Heisenberg CP, Beuchle D, Grandel H, van Eeden FJ, Furutani-Seiki M, Granato M, Haffter P, Odenthal J, Warga RM, Trowe T, Nusslein-Volhard C. 1996. Jaw and branchial arch mutants in zebrafish II: anterior arches and cartilage differentiation. Development 123:345–356.

Piotrowski T, Ahn DG, Schilling TF, Nair S, Ruvinsky I, Geisler R, Rauch GJ, Haffter P, Zon LI, Zhou Y, Foott H, David IB, Ho RK. 2003. The zebrafish van gogh mutation disrupts tbx1, which is involved in the DiGeorge deletion syndrome in humans. Development 130:5043–5052.

Reifers F, Walsh EC, Leger S, Stainier DY, Brand M. 2000. Induction and differentiation of the zebrafish heart requires fibroblast growth factor 8 (fgf8/acerebellar). Development 127:225–235.

Ryan AK, Goodship JA, Wilson DI, Philip N, Levy A, Seidel H, Schuffenhauer S, Oechsler H, Belohradsky B, Prieur M, Aurias A, Raymond FL, Clayton-Smith J, Hatchwell E, McKeown C, Beemer FA, Dallapiccola B, Novelli G, Hurst JA, Ignatius J, Green AJ, Winter RM, Brueton L, Brondum-Nielsen K, Scambler PJ. 1997. Spectrum of clinical features associated with interstitial chromosome 22q11 deletions: a European collaborative study. J Med Genet 34:798–804.

Scambler PJ. 2010. 22q11 Deletion syndrome: a Role for TBX1 in pharyngeal and cardiovascular development. Pediatr Cardiol 31:378–390.

Schilling TF, Piotrowski T, Grandel H, Brand M, Heisenberg CP, Jiang YJ, Beuchle D, Hammerschmidt M, Kane DA, Mullins MC, van Eeden FJ, Kelsh RN, Furutani-Seiki M, Granato M, Haffter P, Odenthal J, Warga RM, Trowe T, Nusslein Volhard C. 1996. Jaw and branchial arch mutants in zebrafish I: branchial arches. Development 123:329–344.

Schoenebeck JJ, Keegan BR, Yelon D. 2007. Vessel and blood specification override cardiac potential in anterior mesoderm. Dev Cell 13:254–267.

Srivastava D, Olson EN. 2000. A genetic blueprint for cardiac development. Nature 407:221–226.

Thisse C, Thisse B, Schilling TF, Postlethwait JH. 1993. Structure of the zebrafish snail1 gene and its expression in wild-type, spadetail and no tail mutant embryos. Development 119:1203–1215.

Vincent SD, Buckingham ME. 2010. How to make a heart: the origin and regulation of cardiac progenitor cells. Curr Top Dev Biol 90:1–41.

Vitelli F, Morishima M, Taddei I, Lindsay EA, Baldini A. 2002a. Tbx1 mutation causes multiple cardiovascular defects and disrupts neural crest and cranial nerve migratory pathways. Hum Mol Genet 11:915–922.

Vitelli F, Taddei I, Morishima M, Meyers EN, Lindsay EA, Baldini A. 2002b. A genetic link between Tbx1 and

fibroblast growth factor signaling. Development 129:4605–4611.
Vitelli F, Lania G, Huynh T, Baldini A. 2010. Partial rescue of the Tbx1 mutant heart phenotype by Fgf8: genetic evidence of impaired tissue response to Fgf8. J Mol Cell Cardiol 49:836–840.
Witzel HR, Jungblut B, Choe CP, Crump JG, Braun T, Dobreva G. 2012. The LIM protein ajuba restricts the second heart field progenitor pool by regulating Isl1 activity. Dev Cell 23:58–70.
Xu H, Morishima M, Wylie JN, Schwartz RJ, Bruneau BG, Lindsay EA, Baldini A. 2004. Tbx1 has a dual role in the morphogenesis of the cardiac outflow tract. Development 131:3217–3227.
Xu H, Cerrato F, Baldini A. 2005. Timed mutation and cell-fate mapping reveal reiterated roles of Tbx1 during embryogenesis, and a crucial function during segmentation of the pharyngeal system via regulation of endoderm expansion. Development 132:4387–4395.
Yagi H, Furutani Y, Hamada H, Sasaki T, Asakawa S, Minoshima S, Ichida F, Joo K, Kimura M, Imamura S, Kamatani N, Momma K, Takao A, Nakazawa M, Shimizu N, Matsuoka R. 2003. Role of TBX1 in human del22q11.2 syndrome. Lancet 362:1366–1373.
Yelon D, Horne SA, Stainier DY. 1999. Restricted expression of cardiac myosin genes reveals regulated aspects of heart tube assembly in zebrafish. Dev Biol 214:23–37.
Zhang Z, Cerrato F, Xu H, Vitelli F, Morishima M, Vincentz J, Furuta Y, Ma L, Martin JF, Baldini A, et al. 2005. Tbx1 expression in pharyngeal epithelia is necessary for pharyngeal arch artery development. Development 132:5307–5315.
Zhang L, Zhong T, Wang Y, Jiang Q, Song H, Gui Y. 2006a. TBX1, a DiGeorge syndrome candidate gene, is inhibited by retinoic acid. Int J Dev Biol 50:55–61.
Zhang Z, Huynh T, Baldini A. 2006b. Mesodermal expression of Tbx1 is necessary and sufficient for pharyngeal arch and cardiac outflow tract development. Development 133:3587–3595.
Zhou Y, Cashman TJ, Nevis KR, Obregon P, Carney SA, Liu Y, Gu A, Mosimann C, Sondalle S, Peterson RE, Heideman W, Burns CE, Burns CG. 2011. Latent TGF-β binding protein 3 identifies a second heart field in zebrafish. Nature 474:645–648.

Developmental Dynamics